Advanced roll bite models for cold and temper rolling processes

T. Dbouk, P. Montmitonnet, N. Suzuki, Y. Takahama, N. Legrand, T. Ngo, H. Matsumoto

This paper describes on-going efforts made to develop a fast and robust roll bite model for cold and temper rolling processes including a non-circular roll profile and a mixed lubrication model based on lubricant flow and surface asperity deformation models (only Coulomb friction is used in this paper however). First, the existing roll bite models are reviewed in details to understand their physics, their specificities, their differences and their resolution strategies, with a particular focus on strategies allowing for short computing time (CPU) even for heavily deformed non circular roll profiles. From this preliminary analysis, some existing strategies are selected to develop a new roll bite model. It includes in particular calculation of roll surface circumferential displacements for roll profile determination and an efficient relaxation technique that updates the relaxation factor dynamically at each roll-strip coupling iteration. The resulting computing time is generally less than one second (on a single processor) and convergence has been obtained for all types of cold and temper rolling conditions, from tandem mill heavy reductions to double reduction of very thin strips and to very light reduction temper rolling (< 0.5%). Simulation results are also discussed against finite element (FE) results. Finally, it is illustrated how this new roll bite model can be used on an industrial database to develop accurate presets of roll force for temper mills.

Keywords: Cold rolling - Temper rolling - Thin strip - Roll bite model - Friction - Mixed lubrication

INTRODUCTION

On industrial cold and temper rolling mills, rolling thin hard strips proves very sensitive to friction. Roll bite models including a lubrication model for precise and local friction determination, together with non-circular roll profile, are of particular interest to take into account friction variation with rolling speed or on-line setup systems like flexible lubrication [1]. For these applications, accurate solutions of the roll bite are needed within a fraction of a second. However, sophisticated roll bite models are generally costly in computing time, while simplified ones perform poorly under extreme rolling conditions and/or over a wide range or

T. Dbouk, P. Montmitonnet

CEMEF, MINES ParisTech and CNRS, France

N. Suzuki, Y. Takahama

Nippon Steel & Sumitomo Metal Corporation, Japan

N. Legrand, T. Ngo

ArcelorMittal Research, France

H. Matsumoto

Univ. Kitakyushu, Japan

rolling conditions (light gauges or/and hard strips and/or high friction and/or large rolls diameters). The aim of this work is to develop a fast and robust roll bite model for cold and temper rolling processes, including mixed lubrication model (lubrication, asperity deformation) and non-circular roll profile. In the present paper however, the presentation is restricted to standard Coulomb friction for more clarity; the lubrication model, its coupling and some applications will be presented elsewhere.

STATE OF THE ART

Many 2D "dry" rolling models have been developed over the past eighty years to predict roll bite contact stresses but also roll force, torque or forward slip during cold rolling. Quoting only milestones, von Kármán [2] introduced the slab method, Orowan [3] drew attention on the effect of shear terms, neglected in the slab method. Bland & Ford [4] assumed a circular deformed work roll profile based on Hitchcock's approach [5], but added the elastic inlet and exit zones which are particularly important e.g. for temper rolling. Grimble et al. [6] and Quan [7] developed models with non-circular work roll profile based on Jortner's influence function (IF) model [8]. In [7], an analysis is made of the role of the radial roll surface deformation in predicting accurate pressure distributions between roll and strip, however neglecting the circumferential roll surface

displacement. Grimble et al. [6] improved the influence function technique by considering both normal and shear stress effects on radial work roll surface displacements. For the first time, they computed roll gap solutions displaying elastic deformation regions embedded within usual plastic deformation zones. Together with roller deformation patterns established in the Elasto-Hydrodynamic Lubrication (EHL) area, this inspired Fleck and Johnson [9,10] to give birth to a new family of models, especially for thin foil rolling, dividing the roll bite into five different regions, elastic or plastic, with or without strip/roll slip.

However, the models presented above where not optimized for short computation time; their robustness was also questionable, they sometimes failed to converge for light gauge strips and strongly non circular roll profiles [6-8]. The relatively long computing time comes from the coupling technique used to solve the roll - strip interactions, combined with the elastic-plastic behavior of the strip. For instance, using fixed-point relaxation techniques between roll and strip calculations required small relaxation factors. This was found necessary to make the model go slowly towards the solution, avoiding roll "indentation", i.e. a spurious local growth of the strip thickness within the bite, near the neutral point, due to very high contact stress punching the roll there. Matsumoto and Shiraishi [11, 12] recognized that models could be much faster using an intelligent relaxation technique that updates the relaxation factor dynamically at each iteration to solve the roll-strip coupling, based on analysis of the behavior of the model during the last iterations. They also introduced the "plastic thickness" concept which they used to prevent positive thickness plastic strain rate (i.e. plastic regrowth of strip thickness): they forced a flat roll surface area where regrowth was detected. This model has demonstrated good efficiency in treating extreme rolling conditions in various situations (light gage, light or heavy reductions, high friction...). However, it included approximations in the computation of contact stresses in the neutral zone and in the elastic-plastic behavior of the strip. Moreover, it did not consider roll circumferential displacements, the importance of which has been suggested recently in temper rolling with very light reductions by Krimpelstätter [13].

The objectives of the present work, based on the previous analysis, include:

- the development of a fast (~1 sec.) roll bite model valid for a wide range of rolling operations, taking into account circumferential displacements and calculating rigorously contact stresses in the neutral zone;

- the evaluation of the real importance of circumferential displacements in temper rolling conditions through a comparative analysis with a reference FE rolling model.

PRESENTATION OF THE COLD ROLLING MODEL

Strip deformation

The slab method [2] is used, deformation is assumed (x, z)-plane strain, variations of all mechanical quantities in both z (ND) and y (TD) directions are neglected compared with x direction (RD). In the plastic deformation zone, the plane strain. The material is elastic-plastic, following Prandtl-Reuss behaviour. Von Mises plasticity criterion is used, shear strains being neglected according to the standard Slab Method assumptions. Boundary conditions are given by the strip tension tresses T_1 and T_2:

$$\begin{cases} \sigma_x = T_1 & \text{at entry} \\ \sigma_x = T_2 & \text{at exit} \end{cases} \tag{1}$$

The strip metal behavior is summarized by elastic parameters E_s (Young's modulus) and v_s (Poisson's ratio) and by a work hardening law called SMATCH which describes the yield stress as an oblique asymptote reached through an exponential branch:

$$\sigma_Y(\bar{\varepsilon}_{pl}) = (A + B\bar{\varepsilon}_{pl})(1 - Ce^{-D\bar{\varepsilon}_{pl}}) + E \tag{2}$$

A, B, C, D, and E are constants provided by the user, σ_Y is the current yield stress and $\bar{\varepsilon}^{pl}$ the equivalent plastic strain.

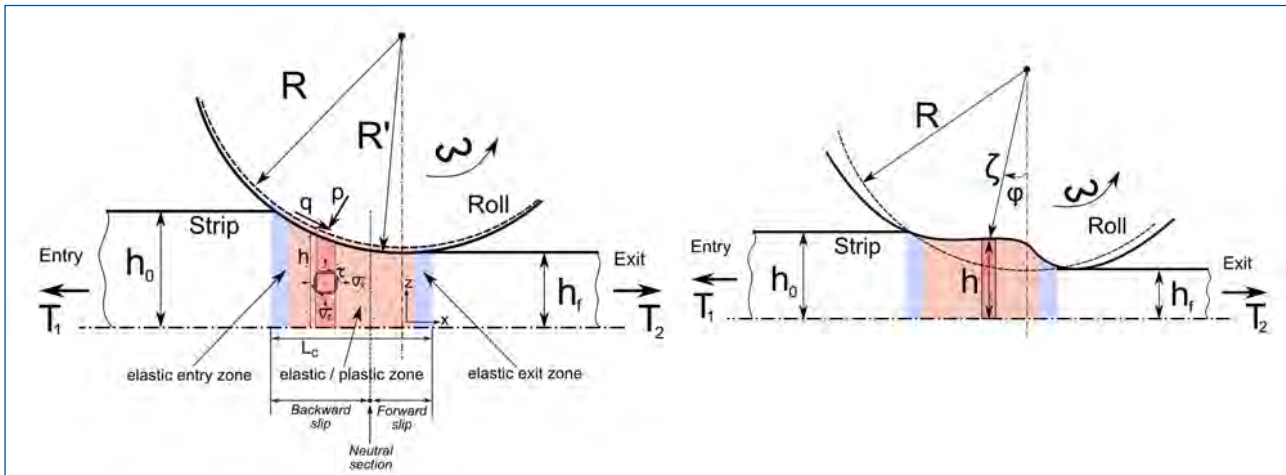All the differential equations of the strip model are solved by a standard Runge Kutta 4th order scheme.

Roll-strip interface

In most models, the discontinuous friction law is regularized (e.g. [11-13]). This means that, noting *Vs* the local sliding velocity, it is made continuous and differentiable at $V_s = 0$. On the contrary, here, the contact between strip and rolls follows pure Coulomb friction with a possibility of sliding or "sticking" (zero relative tangential velocity). Shear stress τ at roll - strip interface is therefore given by [14]:

$\tau = \mu.\sigma_n$ if $V_s \neq 0$ \hfill (3a)

$\tau < \mu.\sigma_n$ if $V_s = 0$ \hfill (3b)

This allows determining accurately those parts of the roll bite where sliding does not take place (the central neutral zone) from the sliding areas (entry and exit). In sliding areas, the friction stress is determined by (3a) using the normal stress resulting from the solution of the equilibrium equation, as in standard slab models. In the "sticking" area, the non-sliding condition controls the local elastic strains, and determines the friction stress ($< \mu.\sigma_n$). Furthermore, a condition $\tau \leq \tau_{max} = \mu.\sigma_Y / \sqrt{3}$ (friction factor model, $\overline{m}$) can be introduced at high normal stress, recalling that anyway, as requested by the plastic yield criterion, $\tau \leq \sigma_Y / \sqrt{3}$. Finally, μ can be made x-dependent, but in the absence of any reliable variation law, this will not be attempted here, this is the purpose of the development of mixed lubrication-based models.

Fig.1 - Cold strip rolling: circular vs non circular work roll deformation

Fig.1 – Laminazione a freddo di nastri: deformazione del cilindro di laminazione circolare vs quello non circolare

Work roll deformation

The non-circular work roll elastic deformation is the result of both radial (u_r) and circumferential (u_θ) work roll displacements [14] due to both normal and tangential load effects, hence 4 terms. Following [8], many authors have neglected the circumferential displacements u_θ. However, results of [13] point to circumferential displacements being important for very light strip reduction, even for the prediction of such global variables as the rolling load and forward slip.

Indeed, starting from the elastic half-space theory [14] for the elastic deformation of a roll surface bounded with a plane surface (i.e. semi-infinite elastic solids) due to both normal and shear stresses,

Jortner et al. [8] proposed a simplification, based on estimates of (u_r) and (u_θ) in "normal" rolling cases. They provided influence functions for determining only $[u_r]_1$ due to the normal stress σ_n distribution along an elementary contact arc of length $2\alpha R$. Their solution is valid strictly for symmetric stress distributions diametrically opposed on the work roll surface (see Fig. 2). Thanks to Saint-Venant's principle and the large roll diameter compared with the contact lengths, it can however be used in strip rolling where the stresses at the roll - strip interface is balanced by a non-symmetrical work roll/ back-up roll stress distribution. The influence function method states that a normal stress distribution concentrated at M_i (a point of contact with the strip) will induce a radial displacement $[u_r]_1$ at another point M_j located at an angle θ from M_i, given by:
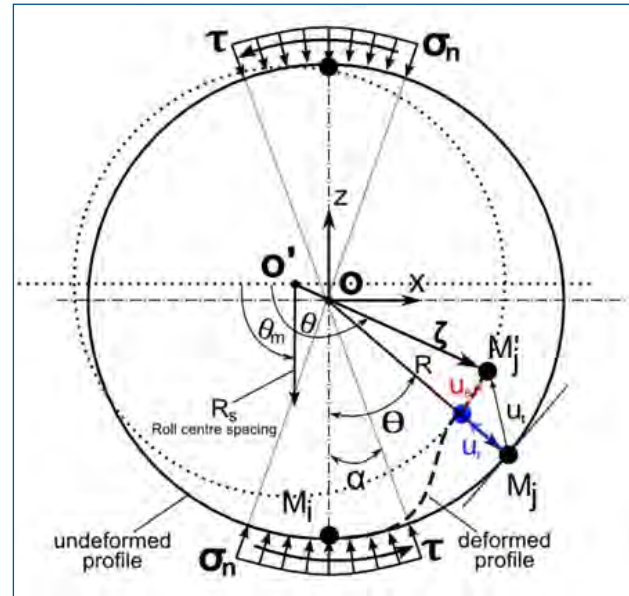
$$[u_r]_1(R, \Theta, \alpha) = \frac{R}{\pi E_r} f(\Theta, \alpha)_1 \cdot \sigma_n \qquad (4)$$

E_r is the work roll Young's modulus, v_r its Poisson's ratio and R the undeformed roll radius. The radial displacement of M_j due to normal stress distribution σ_{ni} can be calculated as:

$$[u_r]_{1j} = \frac{R}{\pi E_r} \sum_{i=1}^{N} f_{ij}(\Theta, \alpha)_1 \cdot \sigma_{n_i} \qquad (5)$$

where $f_{ij}(\theta,a)_1$ are the dimensionless normal influence functions given by:

$$\begin{cases} f_{ij}(\Theta, \alpha)_1 = \frac{1}{2}(v_r - 1)(2 - cos(\Theta - \alpha) - cos(\Theta + \alpha)) \\ + \left(sin(\Theta + \alpha) ln\left(tan^2 \frac{\Theta+\alpha}{2} \right) - sin(\Theta - \alpha) ln\left(tan^2 \frac{\Theta-\alpha}{2} \right) \right) \\ < \Theta < \alpha ; -\pi/2 < \alpha < +\pi/2 \end{cases} \quad (6)$$

Fig. 2 - Radial and circumferential work roll displacement vectors due to rectangular normal and shear stresses distributions (diametrically symmetric) on a contact arc of length $2\alpha R$

Fig. 2 – Vettori dello spostamento radiale e circonferenziale dei cilindri di laminazione dovuto alle distribuzioni delle tensioni normali rettangolari e delle forze di taglio (diametralmente simmetriche) su un arco di contatto lungo $2\alpha R$

Later on, Grimble et al. [6] added to $[u_r]_{1j}$ a second source of radial displacement, the shear stress distribution (τ_i) along $2\alpha R$, $[u_r]_{2j}$, given by:

$$[u_r]_{2j} = \frac{R}{\pi E_r} \sum_{i=1}^{N} f_{ij}(\Theta,\alpha)_2 \cdot \tau_i \qquad (7)$$

where $f_{ij}(\theta,\alpha)_2$ are the dimensionless Golten's shear influence functions [15] given by:

$$\begin{cases} f_{ij}(\Theta,\alpha)_2 = \frac{\pi}{2}(1-v_r)(-sin(\Theta-\alpha) - sin(\Theta+\alpha) + cos(\Theta+\alpha) - cos(\Theta-\alpha)) \\ \quad + \left(\begin{array}{c} -2sin^2\frac{\Theta+\alpha}{2} ln\left(tan^2\frac{\Theta+\alpha}{2}\right) - 2ln\left(cos^2\frac{\Theta+\alpha}{2}\right) \\ -2ln\left(\frac{2}{1+sin(\Theta+\alpha)}\right) + (1-sin(\Theta+\alpha))ln\left(\frac{1-sin(\Theta+\alpha)}{1+sin(\Theta+\alpha)}\right) \end{array} \right) \\ \quad - \left(\begin{array}{c} -2sin^2\frac{\Theta-\alpha}{2} ln\left(tan^2\frac{\Theta-\alpha}{2}\right) - 2ln\left(cos^2\frac{\Theta-\alpha}{2}\right) \\ -2ln\left(\frac{2}{1+sin(\Theta-\alpha)}\right) + (1-sin(\Theta-\alpha))ln\left(\frac{1-sin(\Theta-\alpha)}{1+sin(\Theta-\alpha)}\right) \end{array} \right) \\ \qquad\qquad -\alpha < \Theta < \alpha \, ; \, -\pi/4 < \alpha < +\pi/4 \end{cases} \qquad (8)$$

The total radial work roll displacement u_r due to both normal and shear stresses is:

$$[u_r]_j = [u_r]_{1j} + [u_r]_{2j} \qquad (9)$$

However, both Jortner et al. [8] and Grimble et al. [6] neglected u_θ compared with u_r. As Krimpelstätter [13] has suggested, this might prove insufficient in certain cases (thin strips at very light reductions) and a complete model should take into account both components. The circumferential displacement $([u\theta]_{1j})$ of point M_j due to a normal stress distribution σ_{ni} along $2\alpha R$ (see Figure 3) is calculated as:

$$[u_\theta]_{1j} = \frac{R}{\pi E_r} \sum_{i=1}^{N} f_{ij}(\Theta,\alpha)_3 \cdot \sigma_{ni} \qquad (10)$$

where $f_{ij}(\theta,\alpha)_3$ are dimensionless normal influence functions given by:

$$\begin{cases} f_{ij}(\Theta,\alpha)_3 = \frac{\pi}{2}(v_r - 1)(sin(\Theta+\alpha) + sin(\Theta-\alpha)) \\ \quad -2\left(sin^2\frac{\Theta+\alpha}{2} ln\left(tan^2\frac{\Theta+\alpha}{2}\right) + ln\left(cos^2\frac{\Theta+\alpha}{2}\right)\right) \\ \quad +2\left(sin^2\frac{\Theta-\alpha}{2} ln\left(tan^2\frac{\Theta-\alpha}{2}\right) + ln\left(cos^2\frac{\Theta-\alpha}{2}\right)\right) \\ \qquad\qquad -\alpha < \Theta < \alpha \, ; \, -\pi/2 < \alpha < +\pi/2 \end{cases} \qquad (11)$$

The circumferential displacement $([u\theta]_{2j})$ of point M_j due to shear stress distribution τ_i is:

$$[u_\theta]_{2j} = \frac{R}{\pi E_r} \sum_{i=1}^{N} f_{ij}(\Theta,\alpha)_4 \cdot \tau_i \qquad (12)$$

The dimensionless shear influence functions $f_{ij}(\theta,\alpha)_4$ are given by:

$$\begin{cases} f_{ij}(\Theta,\alpha)_4 = -\frac{\pi}{2}(1-v_r)(-2+cos(\Theta-\alpha) + cos(\Theta+\alpha) + sin(\Theta+\alpha) - sin(\Theta-\alpha)) \\ \quad + \left(-sin(\Theta+\alpha)ln\left(tan^2\frac{\Theta+\alpha}{2}\right) - cos(\Theta+\alpha)ln\left(\frac{1-sin(\Theta+\alpha)}{1+sin(\Theta+\alpha)}\right)\right) \\ \quad - \left(-sin(\Theta-\alpha)ln\left(tan^2\frac{\Theta-\alpha}{2}\right) - cos(\Theta-\alpha)ln\left(\frac{1-sin(\Theta-\alpha)}{1+sin(\Theta-\alpha)}\right)\right) \\ \qquad\qquad -\alpha < \Theta < \alpha \, ; \, -\pi/4 < \alpha < +\pi/4 \end{cases} \qquad (13)$$

The total circumferential work roll displacement can be calculated as:

$$[u_\theta]_j = [u_\theta]_{1j} + [u_\theta]_{2j} \qquad (14)$$

Finally, the vector $\vec{u_{tj}} ((\vec{u_{tj}} = \vec{u_{rj}} + \vec{u_{\theta j}}))$ moves point M_j at (O,R,Θ) to M'_j located at a new polar position (O',ζ, θ) (see Figure 3). Projecting vertically $O'M'_j$ gives the gauge profile of the new deformed work roll that induces a strip thickness modification $2h(\theta)$ given by:

$$2h(\theta) = R_s - 2\zeta(\theta)\cos(\theta - \theta_m) \qquad (15)$$

Rs is the centre spacing between the initial undeformed circular roll and the final new deformed one. In matrix notation, one can write:

$$\begin{bmatrix} [u_r]_j \\ [u_\theta]_j \end{bmatrix} = \frac{R}{\pi E_r} \sum_{i=1}^{N} \left(\begin{bmatrix} f_{ij}(\Theta,\alpha)_1 & f_{ij}(\Theta,\alpha)_2 \\ f_{ij}(\Theta,\alpha)_3 & f_{ij}(\Theta,\alpha)_4 \end{bmatrix} \cdot \begin{bmatrix} \sigma_{ni} \\ \tau_i \end{bmatrix} \right) \qquad (16)$$

The work roll peripheral speed in this modeling is given by:

$$V_r = \omega R \qquad (17)$$

ω is the angular velocity of the work roll of an undeformed radius R.
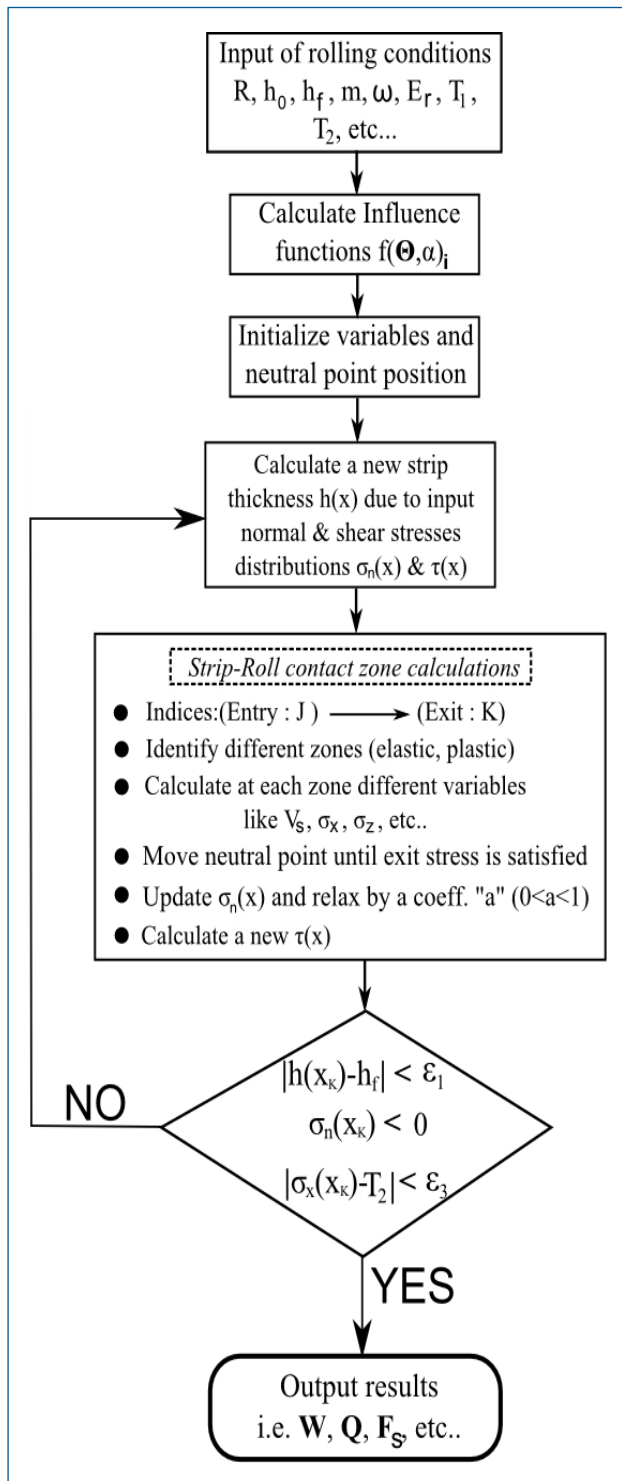
Roll – strip coupling

The global flow chart of the model is shown in fig. 3. It alternates the strip model and the roll model, which is unavoidable since they are not of the same mathematical nature (differential equation on the one hand solved by RK4 technique, matrix-based influence function method on the other hand). It has been amply shown in the literature that in severe rolling cases (thin, hard strip, high friction), this staggered scheme diverges if no precaution is taken. Apart from the Conjugate Gradient model of Grimble et al. [6], all authors use such a coupling with a relaxation technique: before a given iteration, only a part of the stress increase from the previous one is applied in the roll deformation model, so as to slow down the roll shape changes and avoid spurious oscillations. As shown by Matsumoto [10-11], the choice of the relaxation parameter is critical for a robust convergence, and optimal choices can be made for a faster convergence. A similar scheme has been implemented here and its effects will be demonstrated in the following.

ANALYSIS OF CRITICAL FEATURES OF THE MODEL

Impact of work roll circumferential displacements

In this section, the respective values of the 4 influence functions (IF) terms will be analyzed and their impact shown by comparing calculations with and without circumferential displacement, in 4 different cold strip rolling conditions, see Table 1. The first two ones are large reduction rolling of respectively thick (tandem CSM) and thin strips (double reduction), the last two are temper rolling, with 3% reduction on a 0.2 mm strip and 0.36% (very low reduction) on a 0.5 mm thick strip. The strain hardening parameters correspond to a grade really rolled, and the friction coefficients μ have been obtained by fitting experimental values. All the input data are therefore perfectly realistic.

Fig. 3 - A flow chart of the dry cold rolling model computation program.

Fig. 3 – Diagramma di flusso del programma di calcolo del modello di laminazione a freddo e a secco.

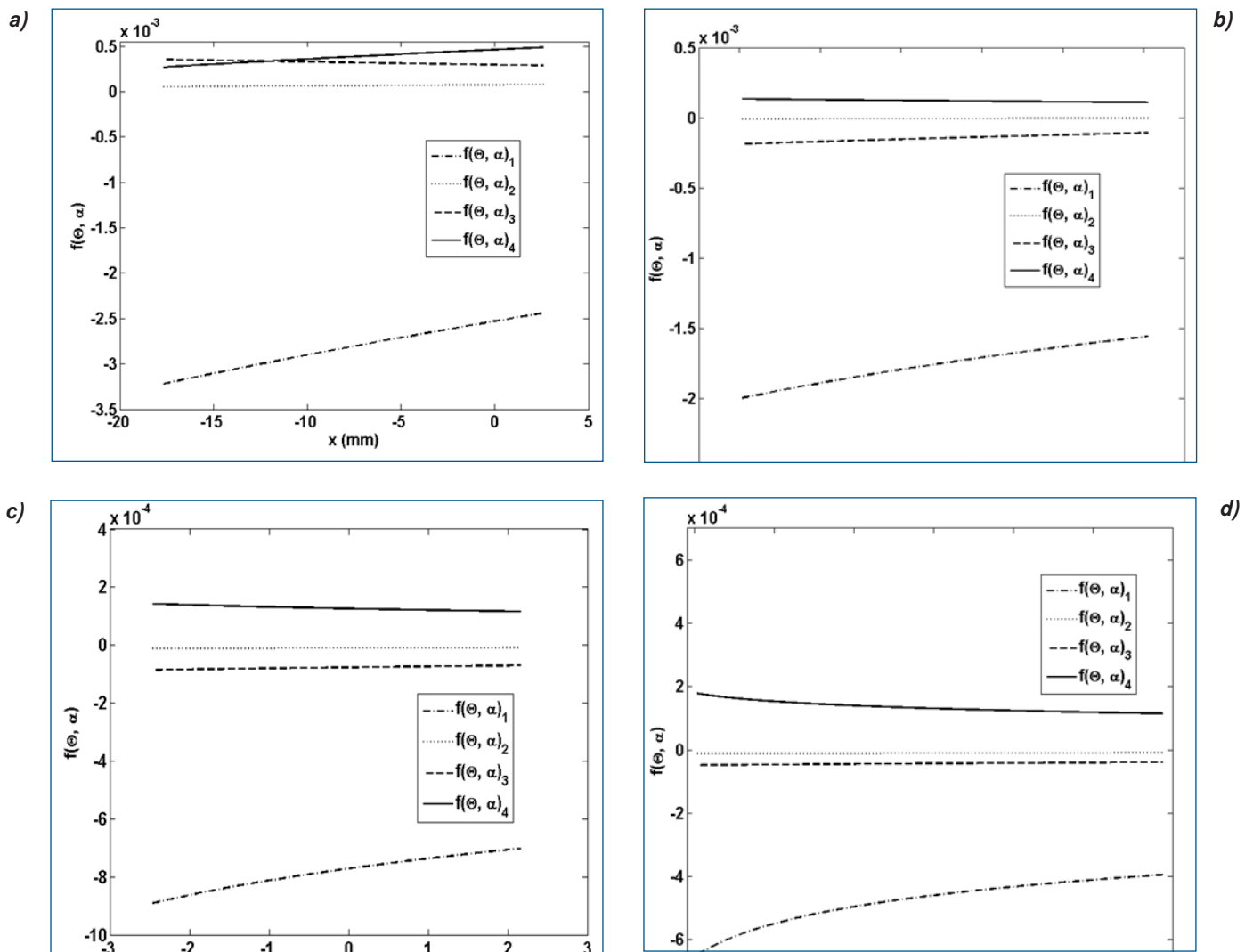| Rolling condition	N° 1	N° 2	N° 3	N° 4
Reduction r	0.355	0.33	0.03	0.0036
$2h_0 : 2h_f (mm)$	3.184 : 2.053	0.2015 : 0.135	0.20 : 0.194	0.5 : 0.4982
$T_1 : T_2 (MPa)$	40 : 120	103.9 : 287.7	98 : 147	25 : 45
$2R(mm)$	526.4	440	480	590
$V_r (mm/sec.)$	3333	18316	18316	18316
$\sigma_Y (MPa)$ [A, B, C, D, E]	[355, 131, 0.3, 11, 0]	[470, 175, 0.45, 8.9, 56]	[0, 0, 0, 0, 340]	[0, 0, 0, 0, 340]
μ	0.075	0.055	0.14	0.25

Table 1 - Four test cases with different cold strip rolling conditions.

Tabella 1 – Quattro casi di prove con diverse condizioni di laminazione di nastri a freddo.

Fig.4 shows the dimensionless IFs. $f(\theta,\alpha)_1$ (normal displacement due to normal stress) is negative and dominates the other ones in all four rolling cases, as expected. $f(\theta,\alpha)_2$ (radial displacement due to shear stress) is almost zero in all cases. As furthermore $f(\theta,\alpha)_1$ is multiplied by a normal stress, much larger than the tangential stress in factor of $f(\theta,\alpha)_2$, it can be concluded that the radial displacement is always largely dominated by $f(\theta,\alpha)_1$, $[ur]_2$ is negligible. $f(\theta,\alpha)_3$ ($u\theta$ due to σ_n) is found to be positive in case N°1 but negative in the other three cases and of the order of 10% of $f(\theta,\alpha)_1$ in magnitude. $f(\theta,\alpha)_4$ is always positive. Its absolute value is generally larger than $| f(\theta,\alpha)_3 |$, so that when it is multiplied by τ, $[u\theta]_1$ and $[u\theta]_2$ might be of similar order, in particular at very light strip reductions (Figures 4c & 4d): both terms must be kept.

Although fig.4 proves that in all cases, $u_\theta << u_r$ ($f(\theta,\alpha)_1$ is about 10 times $f(\theta,\alpha)_3$ and $f(\theta,\alpha)_4$), its effect is non-negligible in cases N°3 and N°4 as seen from Table 2. $u_{\theta j}$ affects significantly the rolling force and the contact length, with a difference of 20% for N°3 and 35% for N°4 (very light reductions, r < 0.5%). Although differences are less than those alleged by [13], this deserves attention. It must be noted however that such a very large influence of circumferential terms is not confirmed by the FEM model described by Hacquin et al. [16] which has been used here for comparison: for rolling condition n°4, FEM roll force is 3951 N/mm with all IF terms and 4115 N/mm with only the radial IF term, the difference is only 4%. [16] use friction regularization, a different IF formulation, and it is a FEM model, hence taking into account shear stresses completely, contrary to the Slab Method. Understanding which of these features leads to this different conclusion is left for future work.

For a detailed comparison, test case N°5 in Table 3 is taken from [13], another very light reduction r = 0.4%. Including u_θ in the present model, with the same IFs as in [13], pressure profiles are very close, while a large difference is found here also if u_θ is neglected. In fact, including u_θ, the model captures better the "friction hill" just beyond the exit to the intermediate neutral zone. This is consistent with the theory of cold rolling of thin foils described by Fleck et al. [10].

a)

b)

c)

d)

Fig. 4 - Dimensionless Influence Functions of test cases of Table 1. a) Case n. 1; b) Case n. 2; c) Case n. 3; d) Case n. 4.

Fig. 4 – Funzioni di influenza adimensionali dei casi di prova in Tabella 1. a) Caso n. 1; b) Caso n. 2; c) Caso n. 3; d) Caso n. 4.

The present model, from fig.5b, predicts slightly less roll deformation than [13] ; note however that the difference is well below 1 μm. Considering the sensitivity of such cases to friction, this might as well be due to the effect of the friction regularization, present in [13] and absent here. - checking its influence is the purpose of next section.
Convergence has been achieved in all these calculations. When 2000 slabs are taken, CPU times are always less than 1 s (Table 2, single CPU at 2.85 GHz).

Regularization of friction law: influence on shear contact stress
The regularization of friction is expected to influence significantly the friction stress, particularly with non-circular roll profiles, because the bite length / strip thickness ratio becomes very large. Test cases N°2 and N°4 are illustrated in fig.6. Fig.6a and fig.6b compare the shear stress given by the present model (non-regularized friction) with

the shear stress from a FEM model [16] with different regularization parameter values. Note that regularization in [16] writes:

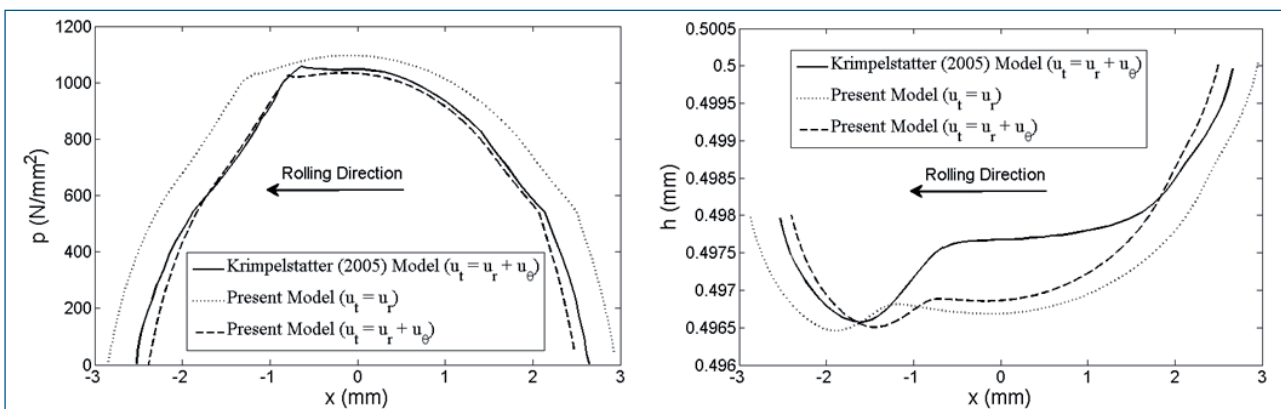$$\tau = \mu.\sigma_n.\frac{V_s}{\sqrt{V_s^2 + (\text{Re}\,g.V_{ref})^2}} \tag{18}$$

where V_{ref} is introduced so that *Reg* is non-dimensional. V_{ref} is taken as 10% of the roll speed; *Reg* is chosen by the user. For case N°2, the shear stress (fig.6b) is little impacted by the regularization, and the normal stress (fig.6c) is very close to the non-regularized present Slab Model. Fig.6a shows how a small, non-zero sliding velocity is however induced by the regularization, while $Vs = 0$ in the neutral zone for the non-regularized case; both Vs profiles converge as *Reg* is reduced.
Temper rolling test case N°4 involves large friction and a

Rolling Results	Red. r	Normalised Mean Rolling Force W (N/mm)	Difference In force w.r.t $\left(\overrightarrow{u_{t_j}} = \overrightarrow{u_{r_j}}\right)$	Forw. Slip Fs (%)	Normalised Mean Rolling Torque Q (N.mm/mm)	Lc (mm)	Time (sec.) 1 CPU 2.85 GHz
N° 1 $\left(\overrightarrow{u_{t_j}} = \overrightarrow{u_{r_j}}\right)$	0.355	8744	-0.32 %	5.01	46459	20.26	0.51
N° 1 $\left(\overrightarrow{u_{t_j}} = \overrightarrow{u_{r_j}} + \overrightarrow{u_{\theta_j}}\right)$		8716		5.05	46244	20.26	
N° 2 $\left(\overrightarrow{u_{t_j}} = \overrightarrow{u_{r_j}}\right)$	0.33	17684	-2.81 %	25.54	7950	10.03	0.99
N° 2 $\left(\overrightarrow{u_{t_j}} = \overrightarrow{u_{r_j}} + \overrightarrow{u_{\theta_j}}\right)$		17187		25.11	7768	9.84	
N° 3 $\left(\overrightarrow{u_{t_j}} = \overrightarrow{u_{r_j}}\right)$	0.03	3858	-19.72 %	2.01	-498	4.61	0.98
N° 3 $\left(\overrightarrow{u_{t_j}} = \overrightarrow{u_{r_j}} + \overrightarrow{u_{\theta_j}}\right)$		3097		1.87	-517	3.92	
N° 4 $\left(\overrightarrow{u_{t_j}} = \overrightarrow{u_{r_j}}\right)$	0.0036	4665	-36.29 %	-0.19	-1282	5.84	0.84
N° 4 $\left(\overrightarrow{u_{t_j}} = \overrightarrow{u_{r_j}} + \overrightarrow{u_{\theta_j}}\right)$		2972		-0.15	-1291	4.26	

Table 2 - Model results for all four rolling test cases of Table 1, including or excluding circumferential $\overrightarrow{u_{\theta_j}}$ displacements .

Tabella 2 – Risultati dei modelli per i quatto casi di prove di laminazione della Tabella 1, inclusi o esclusi gli spostamenti circonferenziali $\overrightarrow{u_{\theta_j}}$.

Fig. 5 - Roll bite under rolling condition N° 5 in Table 3. a) Normal stress profile (case N° 5); b) Strip thickness profile (case N° 5)

Fig. 5 – Cilindro nella condizione di laminazione N° 5 della Tabella 3. a) Normale profilo della tensione (caso N° 5); b) Profilo dello spessore del nastro (caso N° 5)

Rolling condition	N° 5 From Krimpelstatter [14]
Reduction r	0.004
$2h_0 : 2h_f (mm)$	0.5 : 0.4980
$T_1 : T_2 (MPa)$	25 : 43
$2R (mm)$	590
$V_r (mm/sec.)$	6666
$\sigma_Y (MPa)$ [A, B, C, D, E]	[0, 0, 0, 0, 440]
μ	0.15

Table 3 - Temper rolling condition test case N° 5 (from [17]).

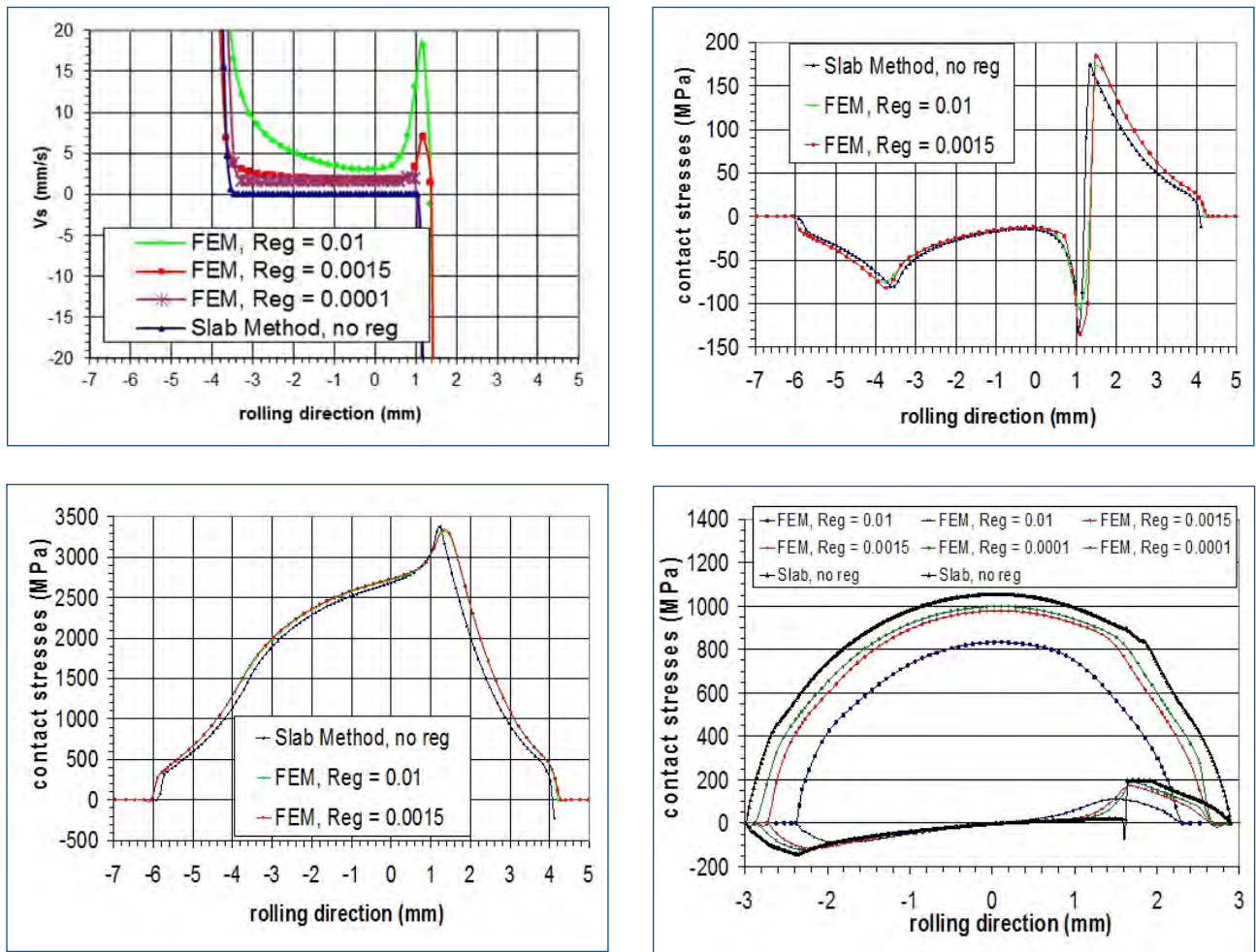*Tabella 3 – Condizioni di finitura del caso di prova N° 5 (da [17]).*

very short roll bite; the deformed roll profile is highly non circular due to the quasi-punctual nature on the contact at the scale of the roll. Decreasing the regularization coefficient Reg, the normal and friction stresses again tend to the non-regularized slab method. However, contrary to test case N°2, choosing too small Reg for better convergence of the FEM solution clearly changes friction, adulterates the normal stress field, and therefore the roll load and torque. A much smaller value of Reg is therefore requested in such cases, with, as a consequence, a larger CPU time due to more iterations (2235 for Reg = 10⁻⁴, versus 816 for Reg = 10⁻², i.e. a 3 times longer calculation).

Fig. 6 - Comparison of shear stress with / without friction regularization for test cases N°2 and 4. a) Case n°2 : sliding velocity; b) Case n°2 : friction stress; c) Case n°2: normal stress; d) Case n°4

Fig. 6 - Confronto fra sforzo di taglio con / senza regolazione dell'attrito per i casi di prova N°2 e 4. a) Caso n°2 : velocità di scorrimento; b) Caso n°2 : tensione di attrito; c) Caso n°2: tensione normale; d) Case n°4

Roll-strip loop dynamic relaxation: importance for CPU time

Following the work of Matsumoto [12], a dynamic relaxation coefficient $a(\gamma)$ was implemented in the relaxation technique of the roll pressure $P(x)$. It is based on the evolution of instabilities in $L_c(\gamma)$ with the γ-th (current) convergence step (iteration). $P(x)$ is under-relaxed according to the following scheme:

$$\begin{cases} P^{(\gamma)} = P^{(\gamma-1)} + \left(1 - a^{(\gamma)}\right) \cdot P \\ \quad a^{(2)} < a(\gamma) \leq 1 \; ; \end{cases} \quad (19)$$

The stability criterion on $Lc(\gamma)$ defines the value of $a(\gamma)$ and is given by the following:

• If the convergence step is stable:
$a^{(\gamma+1)} = min(1.5a^{(\gamma)},a^{(1)})$

• If the convergence step is stable:
$a^{(\gamma+1)} = min(0.5a^{(\gamma)},a^{(2)})$

• If the convergence step is stable during 20 consecutive γ-th iterations:
$a^{(\gamma+1)} = min(1.5a^{(\gamma)},1)$

Unstable means a large difference of contact length or load compared with the previous iteration, in particular a sharp drop. Note that whereas $a^{(1)} = 0.5$, $a^{(2)} = 0.01$ were taken by Matsumoto [12], here $a^{(1)} = 0.5$, $a^{(2)} = 0.05$ are chosen. This was found to be the best solution for both robustness and fast convergence. Next are some results for the rolling condition N°4 in Table 1.

Table 4 shows that using a constant relaxation coefficient versus iterations $a(\gamma) = 0.01$ in the temper rolling condition N° 4 of Table 1, CPU time on a single CPU @ 2.85 GHz is 6.62 s, in 1300 iterations. By taking $a(\gamma) = 0.05$, iteration number is divided by 4 and convergence is achieved in 1.67 s (dashed curve in figure 10). If a dynamic relaxation coefficient is used ($a(\gamma)$; $a^{(2)} = 0.01$), for the same rolling condition on the same machine, convergence is achieved in 360 iterations in 1.94 seconds. Using a dynamic relaxation coefficient ($a(\gamma)$; $a^{(2)} = 0.05$) it takes 237 iterations

Rolling condition N°4 Static / Dynamic relaxation	Relax. Coeff. a	Total number of iterations	CPU Time, 2.85 GHz (sec.)
Static	0.01	1300	6.62
Static	0.05	325	1.67
Dynamic	$\left(a = a(Y); \ a^{(2)} = 0.01\right)$	360	1.94
Dynamic	$\left(a = a(Y); \ a^{(2)} = 0.05\right)$	237	0.84

Table 4 - Static versus Dynamic relaxation

Table 4 – Rilassamento statico vs. rilassamento dinamico

		Methodology n°1: analytical model [17] tuned with LAM3 FE model [16] to calibrate a preset force formula with the industrial database				Methodology n°2: RollGap model to calibrate directly a preset force formula with the industrial database			
Grade	Number of coils	Mean error (%)	Std (%)	RMSE (%)	Freq (%)	Mean error (%)	Std (%)	RMSE (%)	Freq (%)
DK31	96	-0.51	15.35	15.36	72.92	-0.52	14.79	14.80	72.92
DK32	582	-0.48	16.46	16.47	69.76	-0.35	15.96	15.96	71.13
P	730	-1.76	22.56	22.63	43.29	-1.71	23.29	23.35	44.66
BH	1574	-0.40	11.37	11.37	82.72	-0.22	10.22	10.22	87.17

ME(%): mean error of all coils in the grade – STD(%): standard deviation of error – RMSE(%): root mean square error – Freq(%): percentage of coils with roll force error between -15% and 15%
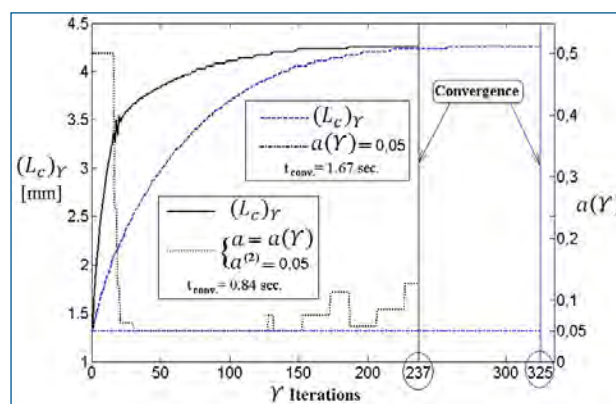
Table 5 - Performance of preset force prediction – comparison of two different methodologies.

Tabella 5 - Attendibilità delle previsioni –confronto tra due diverse metodologie

and 0.84 seconds. Fig.7 displays the $a(\gamma)$ variation versus iterations and its impact on the contact length $Lc(\gamma)$. In the dynamic relaxation mode, around the 20th iteration, an instability occurs in $Lc(\gamma)$ (solid curve) resulting in the algorithm decreasing $a(\gamma)$ from 0.5 to the lower bound 0.05 (dotted curve). However, between the 152th and 172th iterations, $a(\gamma)$ is doubled due to stability in the $Lc(\gamma)$ values over 20 successive iterations.

INDUSTRIAL APPLICATION OF THE MODEL

The present model has been calibrated on an industrial database to derive a simplified formula of roll force prediction for temper rolling with very light reduction, in view of presetting. This methodology n°2 has been compared with an initial methodology (n°1) which uses an analytical simplified model from literature [17]. Table 5 shows that the two methodologies performance is very similar. However with the initial methodology n°1, the different coefficients of the analytical model need to be tuned with a series of ˜1000 FE simulations (˜ 30 min per simulation) for each new industrial database, e.g. new industrial temper mill. This represents a huge computing time of ˜ 500 hours per database. Once this has been done, the calibration of the preset force formula with the tuned analytical model is very quick, because the computing time of the analytical model is almost zero (<< 1 sec.). Methodology n°2 using the present model has the advantage to avoid the preliminary FE tuning: the preset force formula is directly tuned with the present slab model (˜1-10 s per simulation), a significant CPU time saving for a similar preset performance.

Fig. 7 - Sensitivity of Lc(γ) to a(γ) (rolling condition N° 4)

Fig. 7 - Sensibilità di Lc(γ) a a(γ) (condizione di laminazione N° 4)

CONCLUSION AND PERSPECTIVES

A new 2D dry cold rolling model has been developed, including a non-circular work roll profile with influence functions expressed in polar coordinates. To make it possible to investigate very precisely the sliding / sticking status of the neutral zone, in particular in test cases which are very sensitive to the details of the friction stress profile, a non-regularized friction law has been selected. As CPU time is of importance, a dynamic relaxation technique has been used in the strip / roll deformation loop. Inspired by Matsumoto [10, 11], it constitutes an improvement over most models in the literature. Tested under a variety of rolling conditions, the new model has been found robust and fast, resulting in less than 1 s CPU time on a single core,

2.85 GHz computer.

Circumferential displacements have been included in the elastic roll deformation model, a more rigorous approach compared with most models. This allows taking all four terms: radial and circumferential displacements under both normal and tangential stress components; terms may be omitted for a parametric study. A first conclusion is that the radial displacement is insensitive to the tangential stress: the term $f(\theta,\alpha)_2$ may be omitted. In large reduction test cases, only $f(\theta,\alpha)_1$ (radial displacement due to normal stress) needs to be taken into account. However, in accordance with Krimpelstätter [13], circumferential terms are found essential when dealing with very low reduction test cases. It must however be noted that a FEM model using also all 4 IF terms [16], but formulated differently, confirms the existence of an influence of circumferential terms, but finds it much smaller: this point, important for temper rolling, deserves mode attention.

Another point of importance for highly friction-sensitive cases is the impact of the friction threshold regularization applied in most models. They do change the physical nature of friction in order to solve a mathematical difficulty. It is shown here that the details of the friction stress profile may be changed significantly (and so is the tangential velocity profile). Again, for large reduction test cases, the practical impact is low, but when it comes to very low reduction, with by nature very small sliding, the model shows high sensitivity. This point also deserves more work. It must be noted that it is hard to tell, on physical grounds, if mathematically pure non-regularized friction law should be preferred to a regularized friction law.

Seeing the differences between the present Slab Model and the FEM results, it should also be born in mind that the treatment of volumic shear stress is different: the Slab Method completely neglects it, whereas it is naturally involved in the FEM formulation. It is not clear if, in the low reduction cases, shear extends far below the surface and may contribute to decrease the other stress component, including the normal stress. This also should be investigated in the future. Orowan's model provides an elegant, although approximate way to include shear in the Slab Method, as done e.g. in [10, 11].

Finally, implementation of a mixed regime lubrication model is on its way, based on W.R.D. Wilson's ideas (see Chang et al. [18], Marsault et al. [19] or Qiu et al. [20]. Progress will be reported in future papers.

ACKNOWLEDGEMENT

REFERENCES

1]   M. LAUGIER, M. TORNICELLI, C. SILVY LELIGOIS, D. BOUQUEGNEAU, D. LAUNET, J.A. ALVAREZ, Flexible Lubrication concept, the future of cold rolling lubrication. Proc. ICTMP 2010 (Nice, June 13-15th, 2010). E. Felder & P. Montmitonnet, Editors. Transvalor - Presses des Mines, Paris (2010) pp. 735-744.

2]   T. VON KÁRMÁN, Beitrag zur Theorie des Walzvorganges. Z. Angew. Math. Mech. 5, (1925) p.139.

3]   E. OROWAN, Graphical calculation of roll pressure with the assumptions of homogeneous compression and slipping friction. Proc. Inst. Mech. Engrs 150, (1943) p.141.

4]   D.R. BLAND and H. FORD, The calculation of roll force and torque in cold strip rolling with tensions. Proc. Inst. Mech. Engrs 159, (1948) p.144.

5]   J. H. HITCHCOCK, Roll Neck Bearings, Report of ASME Research committee (1935).

6]   M.J. GRIMBLE, M.A. FULLER and G.F. BRYANT, A non-circular arc roll force model for cold rolling, Int. J. Num. Methods Engng 12, (1978) p.643.

7]   Z. QUAN, Deformation characteristics of the cross shear cold rolling (CSCR) of ultra-thin strip and the theory of the "Elastic Plug", Proc. Adv. Technol. Plastic. 2 (1984) p.1173.

8]   D. JORTNER, J.F. OSTERLE and C. F. ZOROWSKI, An analysis of cold strip rolling, Int. J. Mech. Sci. 2 (1987) pp. 179-194.

9]   N.A. FLECK and K.L. JOHNSON, Towards a new theory of cold rolling thin foil, Int. J. Mech. Sci. 29, 7, (1987) pp. 507-524.

10] N.A. FLECK, K.L. JOHNSON, M.E. MEAR and L.C. ZHANG, Cold rolling of foil, Proc. Instn. Mech. Engrs. Vol. 206, (1992) pp. 119-131.

11] H. MATSUMOTO and T. SHIRAISHI, Elastic-Plastic theory of temper rolling with noncircular roll flattening, 49-565, (2008) pp.153-157. In Japanese.

12] H. MATSUMOTO, Elastic-Plastic theory of cold and temper rolling, Proc. 8th Int. Conf. Technology of plasticity, (2005-10), paper No 359.

13] K. KRIMPELSTATTER, Non circular arc temper rolling model considering radial and circumferential displacements, PhD thesis, Linz University, Austria (2005).

14] K. L. JOHNSON, Contact Mechanics. Cambridge University Press, Cambridge (1985).

15] J. W. GOLTEN, Analysis of cold rolling with particular reference to roll deformations, Swansea Doctoral Dissertation, University of Wales (1969).

16] A. HACQUIN, P. MONTMITONNET and J.-P. GUILLERAULT, A steady state thermo-elastoviscoplastic finite element model of rolling with coupled thermo-elastic roll deformation, J. Mat. Proc. Tech. 60 (1996) pp. 109-116.

17] A.J. CARLTON, W.J. EDWARDS, P.J. THOMAS, Formula for Cold Rolling Analysis. Proc. AIME Annual Meeting, 1977, Atlanta, GA, pp 238-248.

18] D. CHANG, N. MARSAULT and W.R.D. WILSON, Lubrication of strip rolling in the low-speed mixed regime, Tribology Trans., 39 (1996) 2, pp. 407-415.

19] N. MARSAULT, P.MONTMITONNET, P. DENEUVILLE and P. GRATACOS, Un modèle de laminage lubrifié en régime mixte, Rev. Met. Sci. Gen. Mat. 98, 5 (2001) pp. 423-433. In French.

20] Z. L. QIU, W. Y. D. YUEN and A. K. TIEU, Mixed-film lubrication theory and tension effects on metal rolling processes, ASME J. Trib 121 (1999) pp. 908-915.

Modelli avanzati di cilindri di laminazione per processi di laminazione a freddo e finitura

Parole chiave: Acciaio - Laminazione – Deformazione plastica

Questo documento descrive gli attuali sviluppi per la creazione di un modello di cilindro di laminazione veloce e robusto per processi di laminazione a freddo e di finitura, ivi compreso un profilo non circolare dei cilindri e un modello di lubrificazione mista basato su ipotesi del flusso di lubrificante e di asperità della superficie di deformazione (comunque in questo documento viene usato solo l'attrito di Coulomb). In primo luogo sono stati rivisti nel dettaglio i modelli dei cilindri di laminazione esistenti per capire i loro aspetti fisici, le loro specificità, le loro differenze e le loro strategie di risoluzione, con particolare attenzione alle strategie che consentono un tempo di elaborazione breve (CPU - short computing time) anche per profili di cilindri non circolari fortemente deformati. A partire da questa analisi preliminare, sono state selezionate alcune strategie esistenti per sviluppare un nuovo modello di cilindro. In particolare quello elaborato comprende il calcolo degli spostamenti circonferenziali della superficie per la determinazione del profilo di laminazione e una tecnica di distensione efficace che aggiorna dinamicamente il fattore di rilassamento ad ogni iterazione dell'accoppiamento cilindro/lamiera. Il tempo di elaborazione risultante è generalmente meno di un secondo (per un singolo processore) e la convergenza è stata ottenuta per tutte le condizioni di laminazione a freddo e temper rolling, dalle forti riduzioni del laminatoio tandem alla doppia riduzione dei nastri molto sottili e alla riduzione molto leggera della finitura (< 0,5 %). I risultati della simulazione sono stati discussi anche rispetto ai risultati del metodo degli elementi finiti (FE). Infine, è stato illustrato come questo nuovo modello per cilindri di laminazione può essere utilizzato in un database industriale per sviluppare programmazioni accurate della forza dei cilindri nei laminatoi di finitura.